九州工業大学学術機関リポジトリ
Kyutacar
Kyushu Institute of Technology Academic Repository

Development of the h-BN manufacturing process for3D-LSI

著者	Yokoi Masashi, Shinkai Satoko, Matsumoto Satoshi
journal or publication title	2021 IEEE CPMT Symposium Japan (ICSJ)
page range	120-121
year	2021-12-24
URL	http://hdl.handle.net/10228/00008801

doi: https://doi.org/10.1109/ICSJ52620.2021.9648854

Development of the h-BN manufacturing process for 3D-LSI

Masashi Yokoi
Department of Advanced Infomatics
Kyushu Institute of Technology
Fukuoka, Japan
q232090m@mail.kyutech.jp

Satoko Shinkai
Department of Advanced Infomatics
Kyushu Institute of Technology
Fukuoka, Japan
shinkai@phys.kyutech.ac.jp

Satoshi Matsumoto
department of Electrical Engineering and Electronics
Kyushu Institute of Technology
Fukuoka, Japan
smatsu@ele.kyutech.ac.jp

Abstract— Hexagonal-BN (h-BN) based SOI structure with through silicon via (TSV) shows higher heat dissipation performance without degrading electrical characteristics compared with the conventional SOI structure. This paper evaluates the manufacturing process for 3D-LSI concluding h-BN. Hexagonal-BN etched by F_2＋He shows useful top shapes of TSV for the 3D-LSI .

Keywords—Hexagonal-BN (h-BN), through silicon via (TSV), dry etching technology, F2+He gas

I. INTRODUCTION

In order to expand "Moore's law", a technology for integrating multiple chips into one package has appeared. A package composed of multiple chips requires (1) smaller external dimensions, (2) higher operating frequency and bandwidth, (3) higher power efficiency, and (4) lower manufacturing costs. To achieve these goals, we expect Three Dimensional-Large Scale Integrated circuits (3D-LSI) using Through Silicon Via (TSV). For the 3D-LSI, exhaust heat is one of the important issues. Then, it is considered to use thin diamond film as an insulator. It has been proposed because the diamond have higher thermal conductivity than SiO_2[1, 2]. But it was only about half of exhaust heat effect which is expected from the thermal conductivity of the nano-crystalline diamond[3]. The nano-crystalline diamond has a surface roughness of several nanometers and this film cannot cover the surface of the heat source and these prevents the heat transfer from heating element to nano-crystalline diamond. This result reveals that higher thermal conductivity and atomically flat surface are required to obtain higher heat exhaust performance. In such situations, hexagonal-BN (h-BN) is attractive for the buried insulator layer because it has higher thermal conductivity with atomically flat surface (Ra of h-BN < 0.25 nm)[4, 5].

The thermal conductivity of the materials is listed in Table I. When SiO_2 is used for Insulators shown in Figs. 1, the low thermal conductivity of SiO_2 (1.38 [W/(m･K)]) causes serious heat storage problems. However, when h-BN is used as an insulator material, the good horizonal thermal conductivity of h-BN (390 [W/(m･K)]) effectively acts on exhaust heat. Especially, TSV is very effective in the case of h-BN as shown in Fig. 2[6]. For the manufacturing of TSV, it is important to establish dry etching technology for h-BN.

In this paper, we have succeeded at patterning h-BN for 3D-LSI manufacturing process, and report the results.

TABLE I. Thermal conductivities

material	Thermal conductivity [W/(m・K)]	
Si	145	
SiO2	1.38	
h-BN	Vertical	2
	Horizonal	390

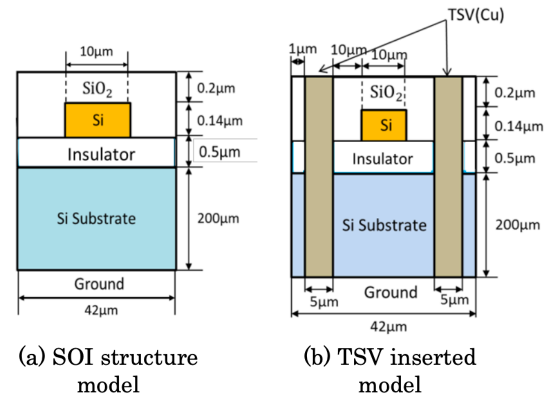

Figs. 1 Schematic of the cross-sectional SOI structure.

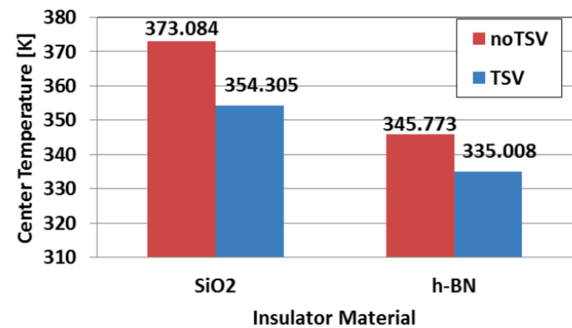

Fig. 2. Temperature at center of heat source (Si) and insulator with and without TSV.

II. EXPERIMENTAL

The sample was used h-BN transferred onto a Si wafer. First, the sample was performed ultrasonic cleaning with pure water for 1 [min]. And then, Al with thickness of 200 [nm] was deposited to form a metal mask. Next, the sample was carried out pattering using a mask-less exposure system (MLA100). The prepared mask patterns were Line & Space type. The width of mask parts (line parts) and etching parts (space parts) were 10 μm and 30 μm, respectively. Inductive Coupled Plasma Reactive Ion Etching (ICP-RIE) was applied for etching method. Fluorine+ helium (F_2:He=1:9),

XXX-X-XXXX-XXXX-X/XX/$XX.00 ©2021 IEEE

CHF_3 and SF_6 were used as the etching gas. The etching conditions were the ICP power of 300 [W], the bias power of 100 [W], the process pressure of 1 [Pa], the gas flow rate of 20 [sccm], and the etching time of 10 [min]. The resist and metal mask ware removed from the sample after ICP-RIE process. The h-BN samples are observed by optical microscope and Scanning Electron Microscopy (SEM).

III. Results and Discussion

Figure 3(a) shows the surface of the h-BN transferred onto Si. From this figure, crystal pattern of the h-BN can be confirmed. Line & space patterns were prepared on this sample. Then, ICP-RIE using F_2+He gas was carried out. The obtained results are shown in Figs. 3 (b) and (c). From Fig. 3(b), it can be seen that h-BN remains on the line parts and completely removed by etching on the space parts. In addition, cross-sectional image of Fig. 3(b) is shown in Fig. 3(c). From this figure, Si is subsequently over-etched about 0.2 µm.

Figure 4 shows the schematic images of h-BN etching mechanism by F_2+He gas. As shown in Fig. 4 (a), the shapes of resist are dome-type. First, the both ends of the resist are etched with the progress of etching, as shown in Fig. 4 (b). Along with this, both ends of the Al mask are etched. After the end of etching, the resist is completely etched as shown in Fig. 4 (c). This phenomenon is under the present etching conditions. If the etching conditions such as the bias power and etching time are changed, the resist may be remained. Next, the Al mask is removed by wet etching as the last process. The cross-sectional image of final state is as shown in Fig. 4 (d).

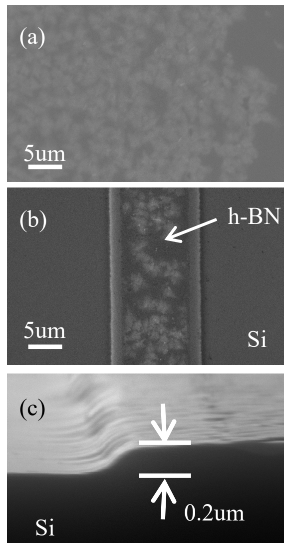

Figs. 3. SEM images of (a) h-BN surface, (b) after dry etching using F2+He gas, (c) cross sectional image of (b)

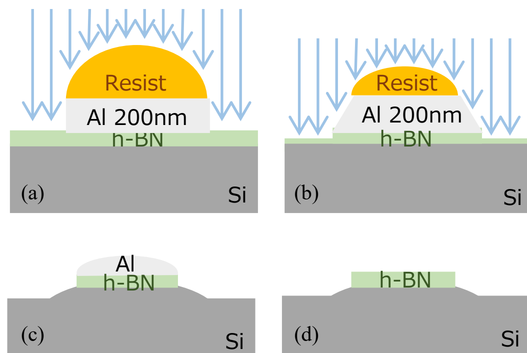

Figs. 4. The schematic images of etching mechanism by F2+He gas :(a) After the start of etching, (b) During etching , (c) After the end of etching, (d) After removing Al mask.

TABLE II. Comparison of etching characteristics

gas	h-BN etching	Isotropic	Anisotropy
F_2+He	Excellent	Poor	Excellent
CHF_3	Fair	Poor	Good
SF_6	Good	Good	Poor

On the other hand, it has been reported that h-BN can be etched using CHF_3 and SF_6 gases. [7,8] Therefore, in order to confirm the usefulness of F_2+He gas for h-BN etching, h-BN etching was performed using CHF_3 and SF_6 gases. As a result, h-BN could not be etched completely in the case of CHF_3 gas. When SF_6 gas was used as etching gas, h-BN was sufficiently etched. However, since SF_6 gas has the property of isotropic, side etching was proceeded strongly. Accordingly, the layout patterns were collapsed. Therefore, it was confirmed that SF_6 gas was unsuitable for h-BN patterning. Table II shows a summary of the etching characteristics of each gas for h-BN.

Therefore, it is found that dry etching of h-BN using F_2 + He gas is a useful etching method to form the top structure of TSV for 3D-LSI.

IV. Conclusion

The h-BN is etched by ICP-RIE using F_2+He, CHF_3 and SF_6 gases. The h-BN cannot be sufficiently etched using CHF_3 gas. When SF_6 gas is used as etching gas, h-BN is sufficiently etched. However, since SF_6 gas has the property of isotropic, side etching is proceeded strongly. Accordingly, the layout patterns were collapsed. Different from these gases, the usefulness of F_2 + He gas for h-BN etching is confirmed. The etching by F_2 + He gas realizes the useful top shapes of TSV for the 3D-LSI .

References

[1] J.-P Mazellier et al., 2009 IEEE Int. SOI Conf. 141, 2009.
[2] K. Nalagawa et al., JJAP vol.53, No.4, 04EP16, 2014.
[3] S. Duangchan et al., J of Material Science; Material in Electronics, vol.28, pp.617-624, 2017.
[4] I. Jo, et al., Nano Lett., 13, 550-554, 2013.
[5] S. M. Kim et al., Nature communications, 6, 8662, 2015.
[6] Yoshiki Sato, Kota Ono, Satoshi Matsumoto, and Masataka Hasegawa, SSDM 2018, pp961-962, 2018
[7] "Dry etching techniques for active devices based on hexagonal boron nitride epilayers", Samuel Grenadier, Jing Li, Jingyu Lin, and Hongxing Jiang, J. Vac. Sci. Technol. A 31(6), Nov/Dec 2013, 06151
[8] ACS Appl. Mater. Interfaces 2020, 12, 8533−8538
[9] S. Grenadier, J. Li, J. Lin, H. Jiang, J. Vac. Sci. Technol. A31(6) 061517, 2013